SUPPLEMENTARY MATERIAL

Appendix 1 – Detailed methodology and additional results of field study

1. Study plot, forest cover and fruit abundance

Field study was conducted at the Sierra de Peña Mayor (43°18’00’’N, 5°30’29’’W, 1000 m a.s.l., Asturias, northern Iberian Peninsula; Supplementary Material Appendix 1 Fig. A1.A). Field sampling was carried out in a rectangular plot of 400 m x 440 m (17.6 ha), chosen to represent a gradient of forest loss, from dense forest patches to pastures with scattered trees. Our plot was subdivided into 440 sampling cells of 20 m x 20 m. This combination of sampling extent and grain is known to adequately represent the spatial scale at which tree regeneration processes operate (from frugivory by birds to seedling survival) (García et al. 2013).

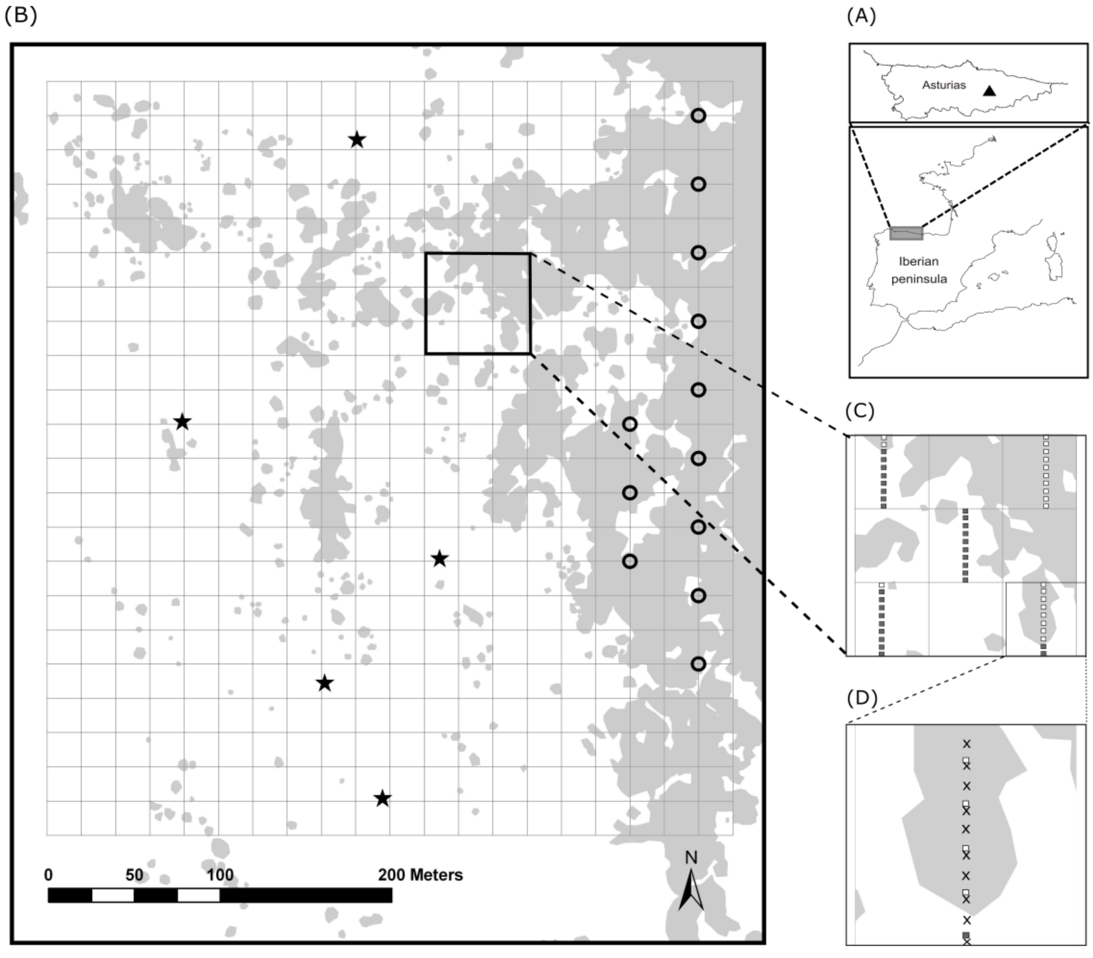

Figure A1 (A) Location of the study site. (B) Scheme of the study plot representing forest cover (gray area) in the 440, 20 m x 20 m sampling cells, as well as the vantage and point-count positions for bird observation (black stars and circles, respectively). (C) A detail of the distribution of seed-rain sampling stations within a subset of cells, which followed a checkered pattern. (D) Detail of a cell showing the distribution of seedling sampling stations located adjacent to seed rain stations (represented by crosses).

In 2009 we developed a Geographical Information System (GIS hereafter; ArcGIS v9.3) based on a recent 1:5000-scale orthophotomap image of the study plot to estimate the percentage of cover per cell (in m^2) after a digitized forest cover layer and the grid of the 440 sampling cells were integrated. We assumed that inter-annual variability in forest cover was insignificant. Additionally, in 2008, 2009, 2010 and 2011, we assessed the position of all individual trees and the fruit crop of each individual fleshy-fruited tree within each cell in order to incorporate data on fruit production into the GIS platform. For this purpose, we visually assigned the standing crop of each individual tree of any fleshy-fruited species by means of a semi-quantitative Fruiting Abundance Index (FAI) using a semi-logarithmic scale (considering six intervals: 0 = without fruits; 1 = 1-10 fruits; 2 = 11-100; 3 = 101-1,000; 4 = 1,001-10,000; 5 > 10,001; Saracco et al. 2005). For each sampling year, we thus included in our GIS platform all data on location, species and FAI of each individual tree. Finally, we calculated the number of trees, as well as the total fruit production per year, per cell, as the sum of the crops of all fruiting trees, both for each individual tree species and for all tree species together. Crop size was extrapolated from FAI ranks following an allometric equation (crop size = 1.77 x $e^{1.92\mathrm{FAI}}$; $R^2 = 0.080$; n = 136 trees, Herrera et al. 2011).

Fruiting tree species showed strong inter-annual variation in fruit crop. For instance, in 2009, it was proportionally higher for *I. aquifolium* than for *C. monogyna*, while in 2010 we found the opposite trend (Fig.2 and Supplementary Material Appendix 1 Fig. A2). Specifically, the number of fruits per square meter per cell for each fruiting tree species (± standard deviation) for 2009 and 2010, respectively, was: *C. monogyna*: 1.44 ± 0.01 and 12.21 ± 0.05; *I. aquifolium*: 14.16 ± 0.06 and 4.81 ± 0.03; *T. baccata*: 1.27 ± 0.02 and 1.77± 0.02. As a result, and taking into account the spatial distribution whereby *I. aquifolium* and *T. baccata* trees are mainly located in forest patches but *C. monogyna* trees are more evenly distributed across the whole study plot (i.e. from larger forest fragments to the deforested matrix), we found a change in the fruiting landscape between years (see also García et al. 2013; Rodríguez-Pérez et al. 2014)

2. Abundance and foraging patterns of frugivorous thrushes

From 2008 to 2011 we recorded the abundance and the foraging behavior of thrushes in our study plot. In order to estimate the abundance, from October to February of each year, we made direct observations from five vantage points located in elevated outcrops (Supplementary Material Appendix 1 Fig. A1.B) in a balanced number of 1-hour observations of all stations. The cumulative yearly observation time was 103, 105, 156 and 215 h (for 2008 to 2011 respectively). Due to the denser forest canopy and topographical characteristics of some stations, complementary bird observations were made from 12 forest point-count positions, each one corresponding to the center of a group of four cells (Supplementary Material Appendix 1 Fig. A1.B). These observations were made over 10 min periods, and the cumulative observation time from each point count was 160, 110, 195 and 230 min (for 2008 to 2011, respectively). For each individual thrush, we recorded the species identity and the sampling cell in which it was observed. Our goal was to provide a measure of bird abundance in functional terms, i.e.

an estimation of the total activity of the frugivorous thrushes across the season in the plot, rather than estimating their actual population sizes. For more information about this methodology, see García and Martinez (2012), García et al. (2013) and Morales et al. (2013).

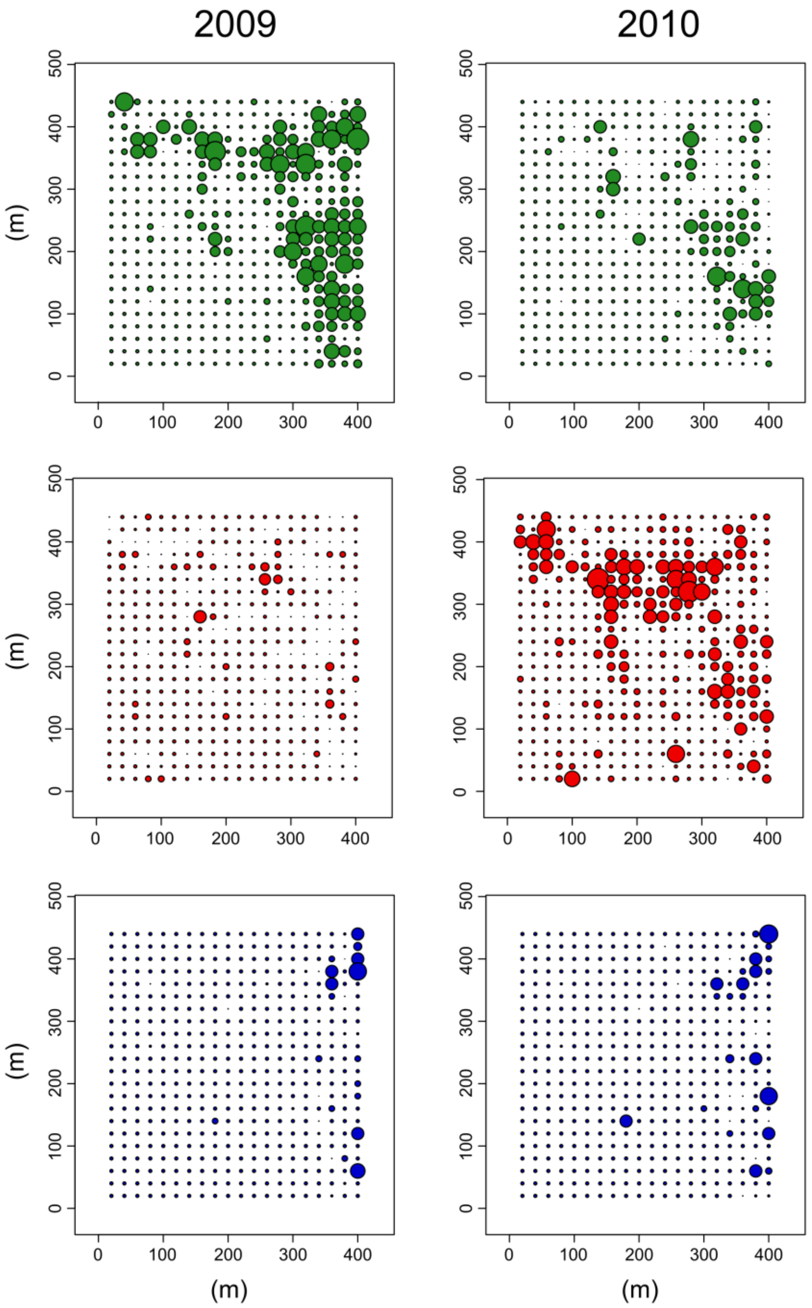

Figure A2. Abundance and distribution of fruit crop of the tree species under study (green: *Ilex aquifolium*; red: *Crategus monogyna*; blue: *Taxus baccata*) in the study plot in two different years (2009 and 2010). Dots represent the centroids of each cell and their size is proportional to the number of fruits per cell.

From 2008 to 2010 we also recorded the foraging behavior and movement patterns of birds in our study plot**.** From October to February, we gathered data on the activity of thrushes over individual sequences from the five vantage positions described above. Observation time was 90, 79 and 63 h for 2008, 2009 and 2010, respectively. During each census time we recorded (a) the thrush species identity, (b) the flight distance of each movement step (i.e. Euclidean distance between the centroids of the starting point and endpoint cells), (c) the duration and the location of resting time (i.e. the perching tree/landing microhabitat), and (d) the species and number of fleshy fruits consumed while perching in a tree. Individual birds were followed until lost, that is, when they disappeared into the canopy and/or left the study plot.

3. Seed dispersal

In fall-winter 2009-2010 and 2010-2011 (sampling years 2009 and 2010, hereafter) we quantified seed deposition by thrushes in a subset of 220 cells following a checkered pattern (Supplementary Material Appendix 1 Fig. A1.C). Along the central longitudinal axis of these cells we set up 10 sampling stations separated from each other by 2 m (Supplementary Material Appendix 1 Fig. A1.B). Each sampling station consisted of a 50 cm x 50 cm open-ground quadrat where all the seeds dispersed by thrushes were collected and counted (Supplementary Material Appendix 1 Fig. A1.C). Seed surveys took place in late November and early January of each sampling year. Each seed sampling station was assigned to one of the following five possible microhabitats, depending on the type of fine-scale cover: (a) under *C. monogyna*, (b) under *I.*

aquifolium, (c) under *T. baccata*, (d) under non-fleshy-fruited species (e.g. *Corylus avellana*) and (e) in the open (i.e. uncovered by tree canopy, e.g. pastures). Thus, we assessed the number of deposited seeds per tree species per year in each sampling station as being the sum of seeds found in the two consecutive surveys.

The germination of the seeds of the studied tree species occurred in the field in the second spring (April to June) following seed dispersal (i.e. after 18 months), with no clear differences between tree species or microhabitat, as suggested by a field germination test conducted in 2004-2005 in an area near the study plot. In this test, sets of 10 seeds recently dispersed by birds and apparently viable (based on checking the fullness of the endocarp by buoyancy) were placed inside 5cm x 5cm glass-fiber bags of 1 mm pore diameter. We buried the seed bags in the topsoil surface layer (at a depth of 3 cm) in 25 sampling stations per each of the following microhabitats: (a) beneath *C. monogyna*, (b) beneath *I. aquifolium*, (c) beneath female *T. baccata*, (d) beneath male *T. baccata* and (e) in the open. After 18 months, we retrieved the bags and in the laboratory counted the number of seeds showing signs of germination (i.e. the seed coat was split into two valves or had seedling remains). Slight differences between microhabitats were found only for seeds of *C. monogyna* beneath *C. monogyna* and in the open, and between tree species with regards to the seeds of *I. aquifolium* and *C. monogyna* in the open (Fig. A3).

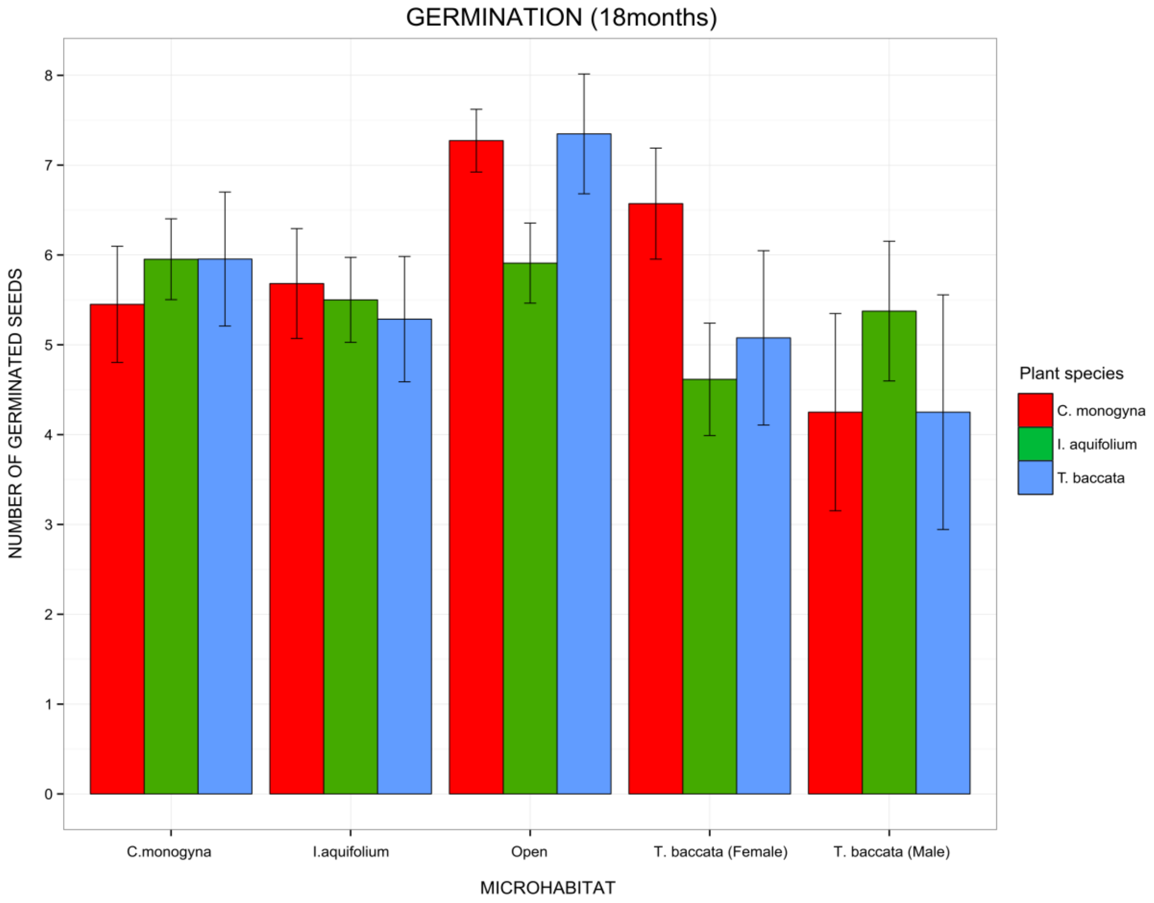

Figure A3. Number of germinated seeds (mean +/- SE) for the different plant species at each of the five microhabitats after a period of 18 months following seed dispersal by birds.

4. Seedling emergence and survival

Seedling emergence and seedling survival surveys took place from April to late August of 2011 and 2012, so that the emerged seedlings corresponded to the cohorts of seeds dispersed in our study site in 2009-2010 and 2010-2011, respectively. We set up five seedling sampling stations distributed in each of the 220 cells, separated by 4 meters from each other but alongside the seed dispersal sampling stations (Supplementary Material Appendix 1 Fig. A1.D). During spring-summer we quantified, with a labeled 50 cm x 50 cm quadrat on the ground, the number of seedlings of each of the three fleshy-fruited tree species of this study which had emerged (*C. monogyna, I. aquifolium* and *T. baccata*). Seedlings were individually identified, by assigning to each of them *x,y* spatial coordinates within the frame of the sampling quadrat, and mapping them on a drawing template. They were aged based on the presence-absence of cotyledons and the stem woodiness (see Peterken and Lloyd, 1967; Thomas and Polwart, 2003). We also determined the microhabitat for each seedling sampling station categorizing them according to the same five microhabitats as for seed sampling stations described above (i.e. under *C. monogyna*, *I. aquifolium*, *T. baccata,* other non-fleshy trees or in open areas). We examined the survival of emerged seedlings monthly during spring and summer, until late August, locating the same individual seedlings across surveys. We considered a seedling to be establishment when it survived until the end of the summer, as previous surveys had revealed that the summer period was the period when most seedling mortality occurred (Martínez 2014).

REFERENCES

García, D. and Martínez, D. 2012. Species richness matters for the quality of ecosystem services: a test using seed dispersal by frugivorous birds. - Proc. Biol. Sci. 279: 3106–13.

García, D. et al. 2013. Functional heterogeneity in a plant-frugivore assemblage enhances seed dispersal resilience to habitat loss. - Ecography 36: 197–208.

Herrera, J.M. et al. 2011. Regional vs local effects of habitat loss and fragmentation on two plant-animal interactions. - Ecography 34: 606–615.

Martínez, D. 2014. Seed dispersal and forest recolonization in a fragmented landscape. Looking for the footprint of thrushes (*Turdus* spp.) beyond the forest. PhD thesis, University of Oviedo. Oviedo.

Morales, J. M. et al. 2013. Frugivore behavioural details matter for seed dispersal: A multi-species model for Cantabrian thrushes and trees. - PLoS One 8: e65216.

Peterken, G. F. and Lloyd, P. S. 1967. Biological Flora of the British Isles*: Ilex aquifolium* L. - J. Ecol. 55: 841–858.

Rodríguez-Pérez J. et al. 2014. Spatial networks of fleshy-fruited trees drive the flow of avian seed dispersal through landscape. - Funct. Ecol. 28: 990–998.

Saracco, J.F. et al. 2005. Crop size and fruit neighborhood effects on bird visitation to fruiting *Schefflera morototoni* trees in Puerto Rico. - Biotropica 37:81–87.

Thomas, P. A. and Polwart, A. (2003). *Taxus baccata* L. - J. Ecol. 91: 489–524.

Appendix 2 – Model details and parameterization of seed rain for five different deposition microhabitats

We adapted the simulation model in Morales et al. (2013) to recreate the relative contribution of each bird species to the total seed rain while moving through a grid-based landscape (see Supplementary Material Appendix 2 Fig. A4). The adapted model includes several rules emulating bird activity and resource tracking. These rules depended on the different spatial behavior of each thrush species and their response to the habitat structure. Thus, they were mainly based on (a) perching time, fruit consumption and gut passage time, (b) movement events and (c) the probability of seed deposition events in different microhabitats. These rules were parameterized for each of the six species of thrushes in order to get a final output: the spatially-explicit and species-specific seed deposition, used to generate a tree-bird seed dispersed interaction matrix.

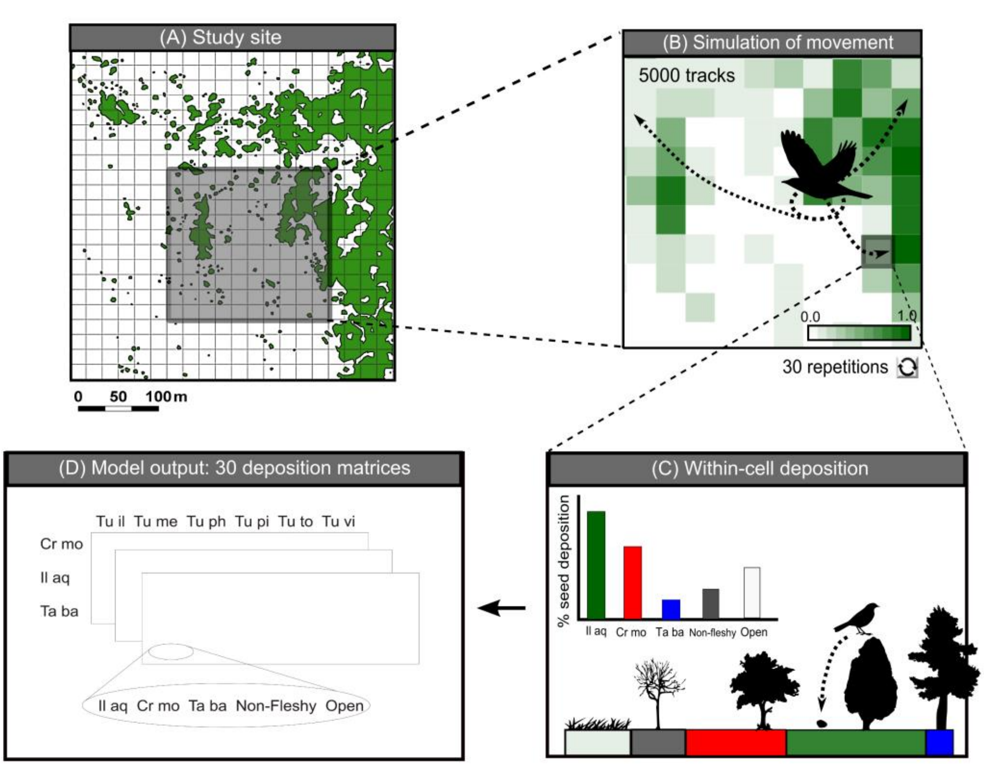

Figure A4. Diagram representing: (A) the distribution of forest cover (green area) in the grid-based study plot divided into cells that replicated the field study plot; (B) a detail showing the proportion of per-cell forest cover represented by the green shading. An example of part of the landscape is plotted with the likely bird movement events and activity (illustrated by arrows). Model simulation is based on 30 replicates of 5000 bird tracks; (C) a schematic representation of the probability of seed deposition events (including the probability of perching in the five microhabitats, and the gut passage time) within a given cell; (D) a final mean simulated tree-bird-microhabitat matrix.

In order to simulate the movement of each bird, our model was fitted to each thrush species based on data obtained from sequences of bird activity made in the study plot from 2008 to 2010 (in which individual birds were tracked by an observer, recording the path followed by the bird and its foraging activity; see Morales et al. 2013). The model aims to predict the seed dispersal patterns that emerge from the interplay between thrush abundance and their response to the spatial heterogeneity of habitat cover and fruit availability. Given the strong inter-annual differences in fruit abundance and distribution typical in this study system (García et al. 2013; see also Supplementary Material Appendix 1, Fig. A2), we used the data of both 2009 and 2010 to fit those model functions related to the number of fruits. The remaining functions, which do not depend on habitat heterogeneity (e.g. distance to the nearest plot border, see below), were fitted also taking into account data from 2008 in order to achieve a bigger sample size.

The calculations described below (i.e. eq. A1, A2, A3 and A4) were used, first, to estimate the values of the parameters needed to build the rules of the mechanistic model. Our mechanistic rules were a combination of mathematical functions describing the performance of each bird species depending on each bird movement, and activity during fruit supply. These mathematical functions had different parameters, i.e. constant values that determined the shape of the function, which varied between thrush species.

The parameters were estimated by fitting different probability density distributions to field data. In other words, the probability that a given event would, (or would not), occur during the activity of each bird (see Supplementary Material Appendix 2 Fig. A5 and Fig. A6). To obtain maximum-likelihood estimates for each parameter, we minimized the negative log-likelihood functions using the Nelder-Mead algorithm (Nelder and Mead 1965) with several overdispersed starting points using the *bbmle* library (Bolker and R Development Core Team 2014). The model was implemented in R statistical language (R Development Core Team 2014). Below we describe the general simulation procedure and how we parameterized the mechanistic rules.

a) Perching time and fruit consumption

Every time a simulated bird arrived to a landscape cell, it spent an amount of time there drawn from a Gamma distribution fitted to the observed perching time for each species. The time a bird was in a given cell was independent of fruit consumption in it, as there is no existing evidence relating to this fact (Morales et al. 2013 and Supplementary Material Appendix 2 Table A1). The decisions of the simulated birds (i.e. to stay or to leave to go to a new landscape cell) were made once perching time expired.

Table A1. Pearson's product-moment correlations between perching time and fruit consumption for each species.

	r	t and df	p - value	CI	
Turdus iliacus	0.084	t = 0.7441, df = 78	0.459	-0.138	0.459
Turdus merula	-0.110	t = -1.0576, df = 91	0.293	-0.307	0.096
Turdus philomelos	0.487	t = 2.494, df = 20	0.021	0.082	0.754
Turdus pilaris	-0.262	t = -0.470, df =3	0.671	-0.929	0.807
Turdus torquatus	-0.426	t = -0.943 , df =4	0.340	-0.920	0.589

Turdus viscivorus	-0.004	t = -0.040, df =86	0.968	-0.214	0.205

Frugivory events depended on both the fruit availability in a given cell and observed fruit consumption rates (García et al. 2013). Simulated birds potentially consumed fruits based on a zero-inflated Poisson distribution fitted to the observed number of fruits consumed by each bird species, and they had no built-in fruit species preferences. Plant species identity depended on fruit species abundance in the landscape cell (Morales et al 2013). If the number of potentially fruits consumed was higher than the number of fruits available in the landscape cell, the simulated birds consumed the minimum between the above-mentioned values.

b) Movement events

When perching time expired, the movements of simulated birds depended on three main decisions, namely whether to: (*i*) stay in the same landscape cell, (*ii*) move to a new cell, or (*iii*) leave the study plot. First, the model computed the probability of leaving the study plot (v) based on the distance to the nearest plot border (B):

$$logit\ (v) = a_0 + b_0B \qquad \textbf{(A1)}$$

where a_0 and b_0 are parameters fitted to each bird species based on observed data. Given that the previous (*i*) rule is independent of habitat heterogeneity (e.g. distance to the nearest plot border, see below), we included the observational data for 2008, with the aim of assuring a larger sample size when fitting the model functions of each bird species.

Second, if simulated birds decided to stay in the plot, their decisions were affected by; (*i*) distance between the current and the destination cell, (*ii*) the proportion of forest cover, and (*iii*) the number of fruits at the destination cell. Thus, the model computed a discrete probability distribution based on hyperbolic tangent functions [*tanh* (*x*)] as follows:

$$\begin{aligned} d_i &= 1 - \tanh\left(\left(\delta_{ij}/a_d\right)^{b_d}\right) \\ c_i &= \tanh\left(\left(\mathrm{cover}_i/a_c\right)^{b_c}\right) \\ f_i &= \tanh\left(\left(\log\left(fruit_i + 1\right)/a_f\right)^{b_f}\right) \\ \mathbf{k} &= \frac{\left[\mathbf{d} \otimes \mathbf{c} \otimes \mathbf{f}\right]}{\sum\left[\mathbf{d} \otimes \mathbf{c} \otimes \mathbf{f}\right]} \end{aligned} \qquad \textbf{(A2)}$$

where the scale (i.e. a_d, a_c and a_f) and shape parameters (i.e. b_d, b_c and b_f) control the shape of the probability between factors. These scale and shape parameters were estimated for each bird species based on observed bird trajectories, forest cover and fruit abundances (Morales et al. 2013). The vectors **d**, **c** and **f** carry the probability of choosing the *i*-th landscape cell depending on the distance to current location (*d*), forest cover (*c*) and fruit abundance (*f*), and they are multiplied in order to achieve a discrete probability vector, **k,** of choosing landscape cells. Once the simulated birds decided where to go, they flew at a constant speed of 6 m s^{-1}, following a straight line and the Euclidean distance from the perch of origin to the destination perch. A maximum number of six movements per track were permitted, as > 95% of sequences recorded in the field were at or below that threshold.

c) Seed deposition events in microhabitats

Furthermore, we implemented the rules to predict seed deposition events into specific microhabitats, as a mechanism combining (*i*) perching probability in the five microhabitats and (*ii*) gut-passage time. The microhabitats considered in the current version were; (*a*) under *C. monogyna,* (*b*) under *I. aquifolium,* (*c*) under *T. baccata*, (*d*) under non-fleshy-fruited tree species and (*e*) in open microhabitat (e.g. pastures)

(Supplementary Material Appendix 2 Fig. A6). For each simulated track and cell, and considering those microhabitats including fleshy-fruited tree species, the perch probability depended on; (1) the foraging activity (based on fruit consumption and movement across the landscape), (2) the number of fleshy fruits in a given cell, and (3) the number of individuals of each tree species in a given cell (Supplementary Material Appendix 2 Fig. A6). The perching probability (k) depending on the number of fruits (B) and trees (C) is thus as follows:

$$\text{logit}(k) = a_o + b_o B + c_o C \qquad \textbf{(A3)}$$

where a_o, b_o and c_o are parameters fitted to each bird species based on observed data. In the case of depositions beneath non-fleshy-fruited trees or in open microhabitat, the perching probability (k) in relation to the number of non-fleshy fruited trees or the proportion of forest cover (B) is as follows:

$$\text{logit}(k) = a_o + b_o B \qquad \textbf{(A4)}$$

where a_o and b_o are parameters fitted to each bird species. For each microhabitat and bird species, we thus obtained estimates from the best model and generated perching probability events based on logistic distributions (Supplementary Material Appendix 2 Fig. A6).

Secondly and based on previous studies in the same area and study system (García et al. 2007), we considered that seeds of a given tree species had a higher probability of arrival beneath the microhabitat representing a tree of that same species (i.e. deposition under conspecifics). We therefore considered the probability of perching in conspecifics (i.e. the same fleshy-fruited species previously consumed) as 0.4, 0.8 and 0.5 for *C. monogyna*, *I. aquifolium T. baccata*, respectively. In essence, this rule mimics a phenomenological matching between the fruiting time of each tree species and its higher perching probability in conspecifics, which may be a consequence of the more limited crop of the other fleshy-fruited species at that time.

For every frugivore event, ingested seeds have a certain gut-passage time (GPT) inside the bird. GPT distributions were fitted to empirical data based on experimental retention times of 18 hand-raised and captive wild specimens of *Turdus merula* (Sobral, Larrinaga and Santamaría, *unpublished data*). GPTs were drawn from a Gamma distribution with a common shape parameter (i.e. 1.59), but a bird species-specific scale parameter (i.e. 0.029 to 0.074; Supplementary Material Appendix 2 Table A2) based on the relationship between the body size and GPT of each *Turdus* species, using eight species from *Turdidae* and *Sylviidae* (Herrera 1984; see Morales et al. 2013).

Table A2. Coefficients of GPT for different species of thrushes based on body size and with reference to *Turdus merula* GPT.

Species	Body size (g)*	mean GPT estimate	Rate for Gamma distribution†
T. iliacus	65	21.45	0.0740
T. merula	100	39.34	0.0400
T. philomelos	75	26.57	0.0598
T. pilaris	110	44.45	0.0357
T. torquatus	120	49.56	0.0320
T. viscivorus	130	54.67	0.0290

* From Collar (2005)

† Assuming the shape parameter is 1.59, the same as in the Gamma distribution fitted to the data from *Turdus merula* in Morales *et al*. 2013.

Finally, seed deposition events in the five microhabitats occurred once frugivory and perching had occurred, and once gut-passage time had expired. Each simulated bird deposited all the seeds consumed in a single deposition event. The number of seeds per deposition was always considered to be one, except for *I. aquifolium*, where the number of seeds deposited was corrected to account for the probability of having between 1 and 4 seeds per fruit, based on Obeso (1998).

d) General considerations and model output

We obtained each model output (i.e. seed deposition data) as a spatially-explicit (cell- and microhabitat-based) prediction of seed deposition for each tree species and by each bird species, that is, a multi-specific seed rain across the modeled landscape. Each model output was the result of a simulation accounting for 5000 bird tracks, and the simulations were replicated 30 times (i.e. 30 independent model outputs), for each of the two different year scenarios (2009 and 2010). These year scenarios accounted for the field-based values of fruit availability and bird abundance of the different species in the respective years. We finally selected the seed deposition output corresponding to a subset of 220 cells of the modeling landscape, in equivalent positions to those containing seed deposition and seedling establishment sampling stations in the field (Supplementary material Appendix 1, Fig. A1.C).

The data of each seed deposition output, accounting for tree-bird and tree-microhabitat specific information, were pooled across microhabitats. In this way we obtained a seed deposition matrix which accounted for the number of seeds of each of the different tree species which were dispersed by each bird species. For each year scenario, we thus obtained 30 matrices of simulated seed deposition (Fig. 1D).

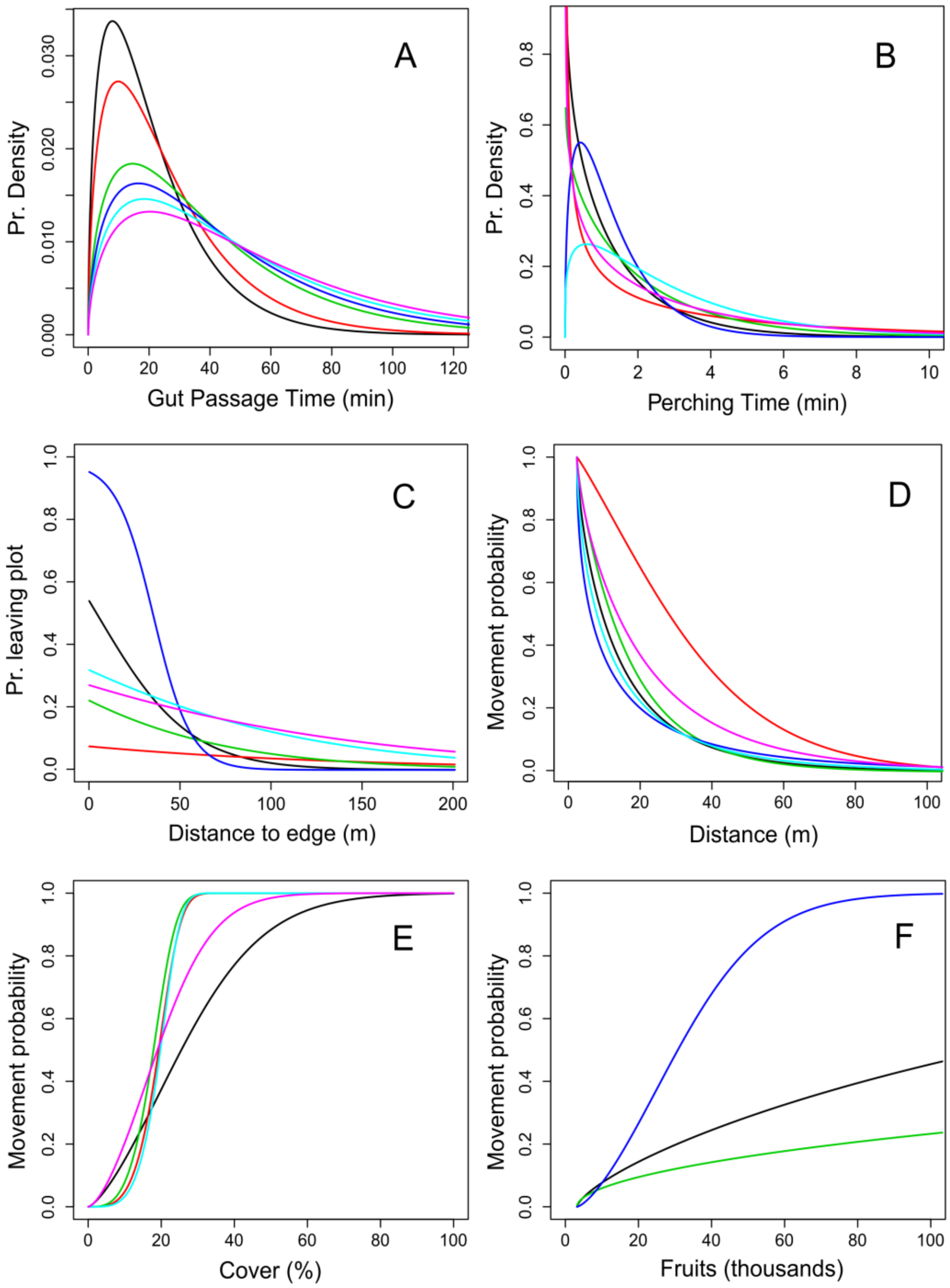

Figure A5. Model functions fitted to different species of thrushes for perching time, movement probabilities and gut-passage time. Gut-passage time (A) is Gamma distributed with scale parameter related to bird size. Perching time (B) is Gamma distributed and fitted to data from direct observations. The probability of leaving the study plot (C) decreased with distance to the plot edge. Movement to another landscape cell (D) decreased with increased distance to that cell. Movement probability increased with forest cover and with fruits (E and F). The species of thrushes are: *Turdus iliacus* (black), *T. philomelos* (red), *T. merula* (green), *T. piralis* (blue), *T. torquatus* (cyan) and *T. viscivorus* (magenta). (A) and (C) were fitted with observational data collected during 2007, 2008, 2009, 2010, as in Morales et al (2013); (B) during 2008, 2009, 2010; and (D), (E), and (F) with observational data collected during 2009, 2010 because they corresponded to functions depending on landscape characteristics and, thus, could vary between years.

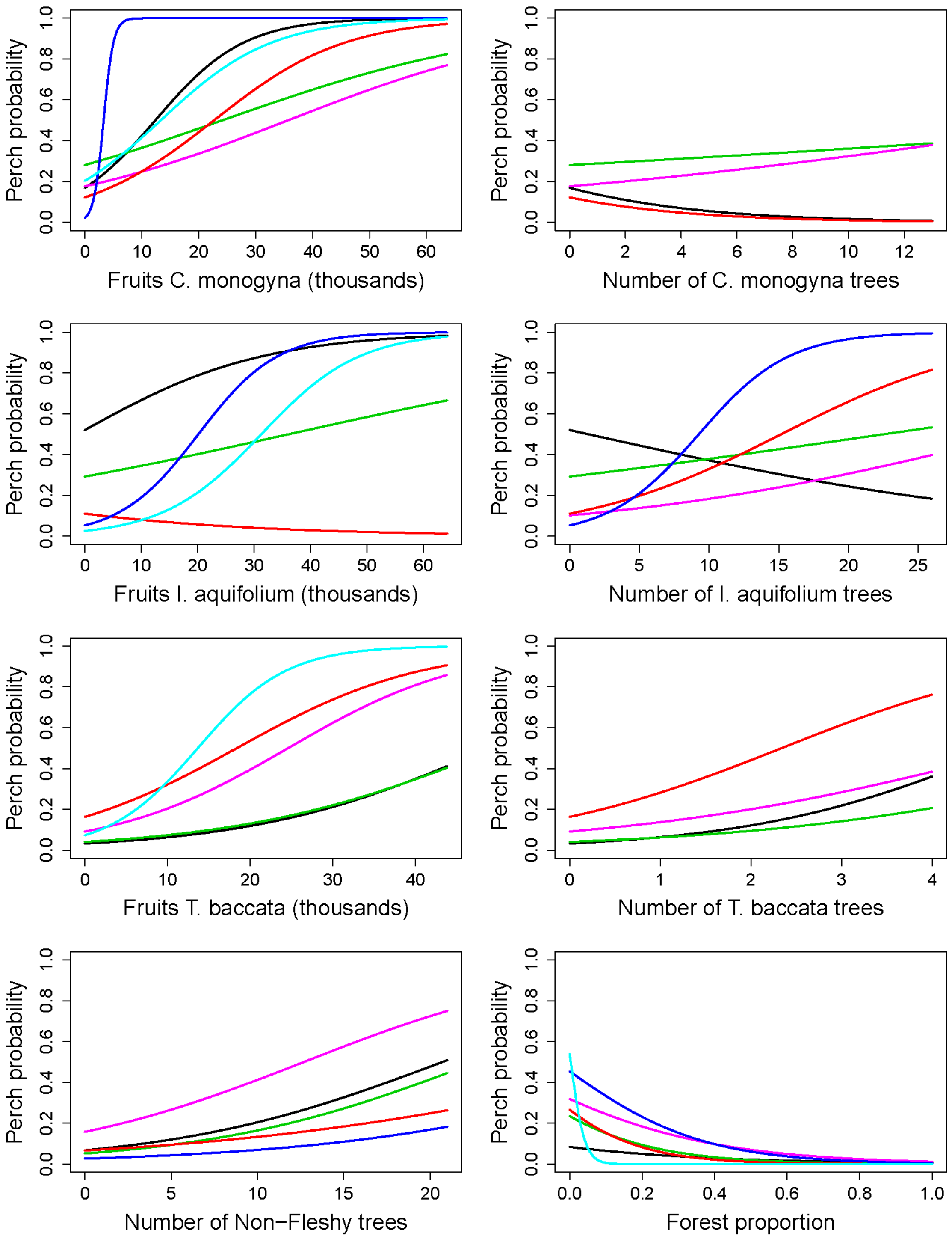

Figure A6. Mechanistic functions describing perching probability beneath microhabitats for each *Turdus* species. For each microhabitat, we calculated perching probability as a function of fruits and number of trees of *C. monogyna* (first row), *I. aquifolium* (second row), and *T. baccata* (third row). For non-fleshy-fruited trees (fourth row, left) deposition probabilities only depended on the number of trees, whereas the probability of deposition in the open (fourth row, right) was calculated as a function of the proportion of forest cover. The *Turdus* species are: *T. iliacus* (black), *T. philomelos* (red), *T. merula* (green), *T. piralis* (blue), *T. torquatus* (cyan) and *T. viscivorus* (magenta).

REFERENCES

Bolker B. and R Development Core Team 2014. *bbmle*: Tools for general maximum likelihood estimation. -R package version 1.0.17. http://CRAN.R-project.org/package=bbmle

Collar, N. J. 2005. Family Turdidae (Thrushes). Pp. 514-807 in del Hoyo, J., Elliot, A. & Christie, D. A. Handbook of the Birds of the World. Vol. 10. Cuckoo-shrikes to Thrushes. Lynx Edicions, Barcelona.

García, D. et al. 2007. Seed transfer among bird-dispersed trees and its consequences for post-dispersal seed fate. - Basic Appl. Ecol. 8: 533–543

García, D. et al. 2013. Functional heterogeneity in a plant-frugivore assemblage enhances seed dispersal resilience to habitat loss. - Ecography 36: 197–208

Herrera, C.M. 1984. Adaptation to frugivory of Mediterranean avian seed dispersers. - Ecology 65: 609–617

Morales, J. M. et al. 2013. Frugivore behavioural details matter for seed dispersal: A multi-species model for Cantabrian thrushes and trees. - PLoS One 8: e65216.

Nelder, J.A. and Mead, R. 1965. A simplex method for function minimization. - *Computer Journal*. 7: 303-313

Obeso, J.R. 1998. Patterns of variation in *Ilex aquifolium* fruit traits related to fruit consumption by birds and seed predation by rodents. - EcoScience 5 (4): 463-469

R Development Core Team 2013. R: a Language and Environment for Statistical Computing. R Foundation for Statistical Computing, Vienna.

Appendix S3 – Matrices

Table A3. Tree-microhabitat observed seed deposition matrices. Relative abundance of seeds (in %) of different tree species (rows) deposited by frugivorous birds in different microhabitats (columns) for 2009 (a) and 2010 (b). The total number of observed seeds per fleshy-fruited tree species under study is specified in the last column.

(a) 2009	Under *C. monogyna*	Under *I. aquifolium*	Under *T. baccata*	Under non-fleshy-fruited tree	Open	No. seeds
Crataegus. monogyna	30.46	40.61	5.31	14.99	8.62	847
Ilex aquifolium	9.58	69.56	2.28	12.69	5.88	32131
Taxus baccata	18.49	27.92	35.89	11.62	6.07	1368

(b) 2010	Under *C. monogyna*	Under *I. aquifolium*	Under *T. baccata*	Under non-fleshy-fruited tree	Open	No. seeds
Crataegus. monogyna	29.75	47.98	4.22	6.53	11.52	3126
Ilex aquifolium	15.46	70.23	6.59	5.09	2.63	9477
Taxus baccata	5.03	24.82	54.17	7.14	8.84	2228

Table A4. Tree-microhabitat first transition probability. *Seedling emergence rates* for the different tree species (rows) in different microhabitats (columns), corresponding to two seed cohorts, 2009 (a) and 2010 (b). *Seedling emergence rates* were calculated as the proportion of dispersed seeds from which a seedling emerged after an 18 months post-dispersal period.

(a) 2009	Under *C. monogyna*	Under *I. aquifolium*	Under *T. baccata*	Under non-fleshy-fruited tree	Open
Crataegus. monogyna	1.000	0.493	0.364	0.370	1.000
Ilex aquifolium	0.117	0.049	0.109	0.100	0.476
Taxus baccata	0.077	0.017	0.017	0.238	0.000

(b) 2010	Under *C. monogyna*	Under *I. aquifolium*	Under *T. baccata*	Under non-fleshy-fruited tree	Open
Crataegus. monogyna	0.789	0.324	0.364	0.622	1.000
Ilex aquifolium	0.192	0.168	0.093	0.809	1.000
Taxus baccata	0.042	0.082	0.008	0.050	0.062

Table A5. Tree-microhabitat second transition probability. *Seedling survival rates* for different tree species (rows) in different microhabitats (columns), corresponding to two seed cohorts, 2009 (a) and 2010 (b). *Seedling survival rates* were calculated as the proportion of emerged seedlings which survived to the end of the summer season.

(a) 2009	Under *C. monogyna*	Under *I. aquifolium*	Under *T. baccata*	Under non-fleshy-fruited tree	Open
Crataegus. monogyna	0.386	0.413	0.250	0.500	0.458
Ilex aquifolium	0.550	0.352	0.461	0.516	0.193
Taxus baccata	1.000	0.500	0.500	0.500	0.000

(b) 2010	Under *C. monogyna*	Under *I. aquifolium*	Under *T. baccata*	Under non-fleshy-fruited tree	Open
Crataegus. monogyna	0.224	0.247	0.125	0.357	0.295
Ilex aquifolium	0.516	0.390	0.500	0.436	0.203
Taxus baccata	1.000	0.143	0.333	0.273	0.000

Table A6. Tree-microhabitat predicted seed deposition matrices. Relative abundance of simulated seeds (in %) of the different tree species (rows) deposited by frugivorous birds in different microhabitats (columns) for 2009 (a) and 2010 (b).

(a) 2009	Under *C. monogyna*	Under *I. aquifolium*	Under *T. baccata*	Under non-fleshy-fruited tree	Open	No. seeds
Crataegus. monogyna	34.76	31.25	11.72	10.94	11.33	256
Ilex aquifolium	2.70	90.73	3.01	2.26	1.30	3227
Taxus baccata	7.32	31.71	43.90	12.19	4.88	41

(b) 2010	Under *C. monogyna*	Under *I. aquifolium*	Under *T. baccata*	Under non-fleshy-fruited tree	Open	No. seeds
Crataegus. monogyna	43.11	22.17	17.20	8.57	8.95	1610
Ilex aquifolium	4.03	87.15	4.50	3.09	1.23	1712
Taxus baccata	9.65	18.42	59.65	8.77	3.51	114

Table A7. Tree-microhabitat predicted seedling recruitment matrices. Relative abundance of simulated seedlings (in %) of the different tree species (rows) recruited by frugivorous birds in different microhabitats (columns) for 2009 (a) and 2010 (b). The total number of predicted seedling recruited per tree species is specified in the last column.

(a) 2009	Under *C. monogyna*	Under *I. aquifolium*	Under *T. baccata*	Under non-fleshy-fruited tree	Open	No. seedlings
Crataegus. monogyna	47.89	22.54	4.22	7.04	18.31	71
Ilex aquifolium	8.69	72.46	7.25	5.80	5.80	69
Taxus baccata	50.00	0.00	0.00	50.00	0.00	2

(a) 2010	Under *C. monogyna*	Under *I. aquifolium*	Under *T. baccata*	Under non-fleshy-fruited tree	Open	No. seedlings
Crataegus. monogyna	52.13	11.97	5.13	12.82	17.95	234
Ilex aquifolium	5.35	74.81	2.29	14.50	3.05	131
Taxus baccata	100.00	00.00	0.00	0.00	0.00	1

Table A8. Bird-microhabitat predicted seed deposition matrices. Relative abundance of seeds (in %) deposited by each of the frugivorous bird species (rows) in the different microhabitats (columns) for 2009 (a) and 2010 (b). The total number of predicted seeds deposited by each bird species is specified in the last column.

(a) 2009	Under *C. monogyna*	Under *I. aquifolium*	Under *T. baccata*	Under non-fleshy-fruited tree	Open	No. seeds
T. iliacus	2.74	93.85	1.27	1.81	0.33	1495
T. merula	8.56	86.24	2.01	1.51	1.68	596
T. viscivorus	10.45	70.65	3.98	9.95	4.97	201
T. philomelos	5.34	78.29	8.74	3.81	3.82	1179
T. pilaris	0.00	94.12	0.00	0.00	5.88	17
T. torquatus	8.57	65.71	8.57	14.29	2.86	35

Table A8 cont. Bird-microhabitat predicted seed deposition matrices. Relative abundance of seeds (in %) deposited by each of the frugivorous bird species (rows) in the different microhabitats (columns) for 2009 (a) and 2010 (b). The total number of predicted seeds deposited by each bird species is specified in the last column.

(b) 2010	Under *C. monogyna*	Under *I. aquifolium*	Under *T. baccata*	Under non-fleshy-fruited tree	Open	No. seeds
T. iliacus	25.54	65.76	3.26	4.35	1.09	184
T. merula	31.60	58.84	2.49	3.95	3.12	481
T. viscivorus	29.10	44.44	6.88	12.17	7.41	189
T. philomelos	19.76	53.87	15.29	5.74	5.34	2545
T. pilaris	50.00	41.67	0.00	0.00	8.33	12
T. torquatus	45.46	27.27	9.09	18.18	0.00	22

Table A9. Bird-microhabitat predicted seedling recruitment matrices. Relative abundance of seedlings (in %) recruited by each of the frugivorous bird species (rows) in the different microhabitats (columns) for 2009 (a) and 2010 (b). The total number of predicted seedlings recruited by each bird species is specified in the last column.

(a) 2009	Under *C. monogyna*	Under *I. aquifolium*	Under *T. baccata*	Under non-fleshy-fruited tree	Open	No. seedlings
T. iliacus	21.28	68.09	2.13	4.25	4.25	47
T. merula	44.45	40.74	3.70	3.70	7.41	27
T. viscivorus	40.00	20.00	0.00	20.00	20.00	10
T. philomelos	25.00	35.72	10.71	8.93	19.64	56
T. pilaris	33.33	33.33	0.00	0.00	33.33	3
T. torquatus	20.00	20.00	20.00	20.00	20.00	5

Table A9 cont. Bird-microhabitat predicted seedling recruitment matrices. Relative abundance of seedlings (in %) recruited by each of the frugivorous bird species (rows) in the different microhabitats (columns) for 2009 (a) and 2010 (b). The total number of predicted seedlings recruited by each bird species is specified in the last column.

(b) 2010	Under *C. monogyna*	Under *I. aquifolium*	Under *T. baccata*	Under non-fleshy-fruited tree	Open	No. seedlings
T. iliacus	44.44	44.44	0.00	11.11	0.00	18
T. merula	49.06	35.85	0.00	7.55	7.55	53
T. viscivorus	37.50	20.83	0.00	25.00	16.67	24
T. philomelos	31.83	34.83	5.62	13.48	14.23	267
T. pilaris	100.00	0.00	0.00	0.00	0.00	1
T. torquatus	66.66	0.00	0.00	33.33	0.00	3